

Supplementary Information

Limitations of conjugated polymers as emitters in triplet-triplet annihilation upconversion

Riley O'shea,^{a,b} Can Gao,^c Siobhan Bradley,^a Tze Cin Owyong,^{a,b} Na Wu,^{a,b} Jonathan M. White,^b Kenneth P. Ghiggino,^a Wallace W. H. Wong^{a,b*}

^aARC Centre of Excellence in Exciton Science, School of Chemistry, University of Melbourne, Parkville, VIC 3010, Australia

^bSchool of Chemistry, Bio21 Institute, University of Melbourne, Parkville, VIC 3010, Australia

^cBeijing National Laboratory for Molecular Sciences, Key Laboratory of Organic Solids, Institute of Chemistry, Chinese Academy of Sciences, Beijing, China

*E-mail: wwhwong@unimelb.edu.au

Contents

1. NMR and mass spectra	2
2. Xray crystallography.....	11
3. Polymerization data	14
4. Density functional theory calculation	15
5. Photophysical data	16

1. NMR and mass spectra

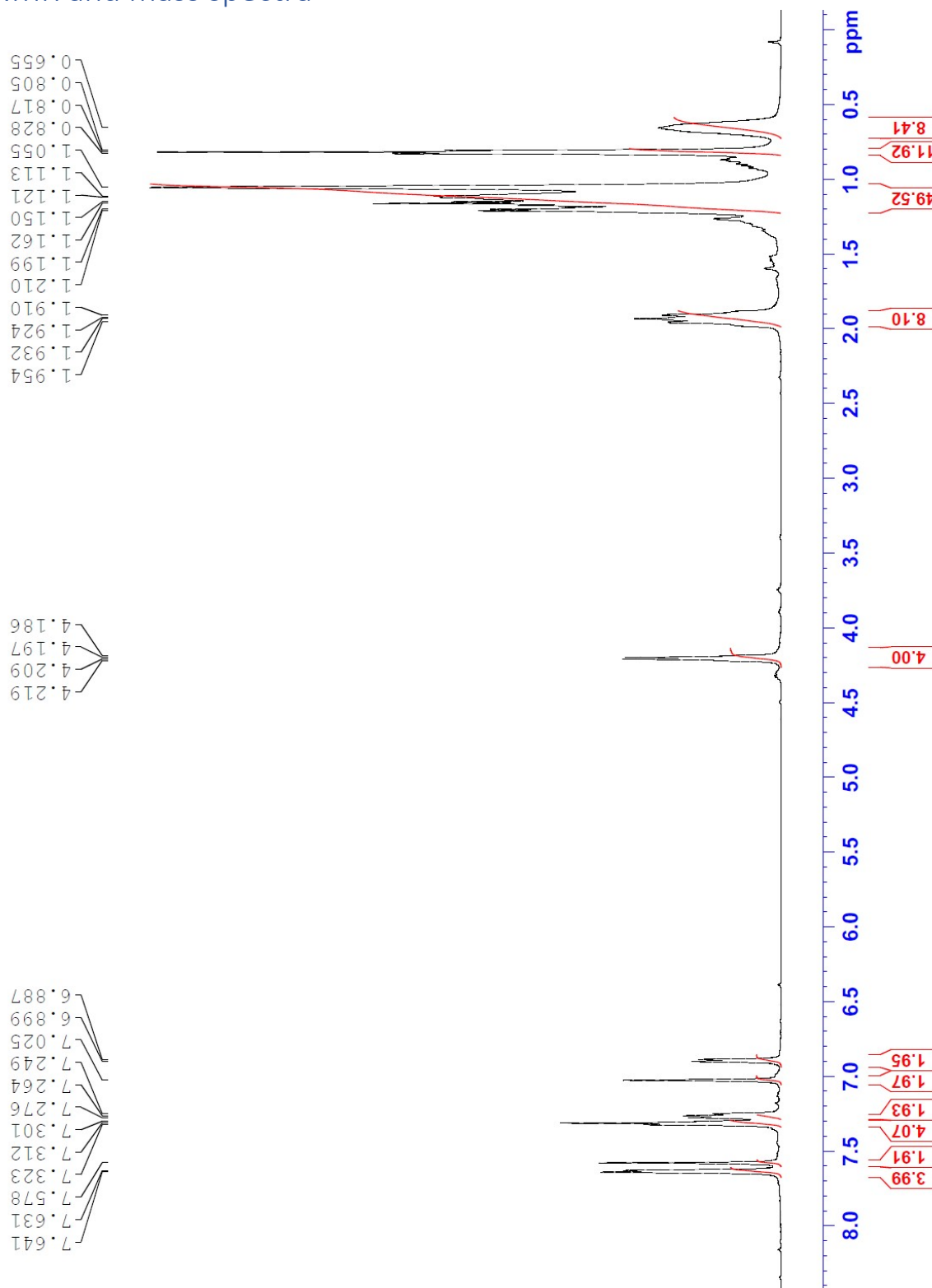


Figure S 1 ¹H NMR spectra of diethyl 2,5-bis((9,9-dioctyl-9H-fluoren-2-yl)oxy)terephthalate 3.

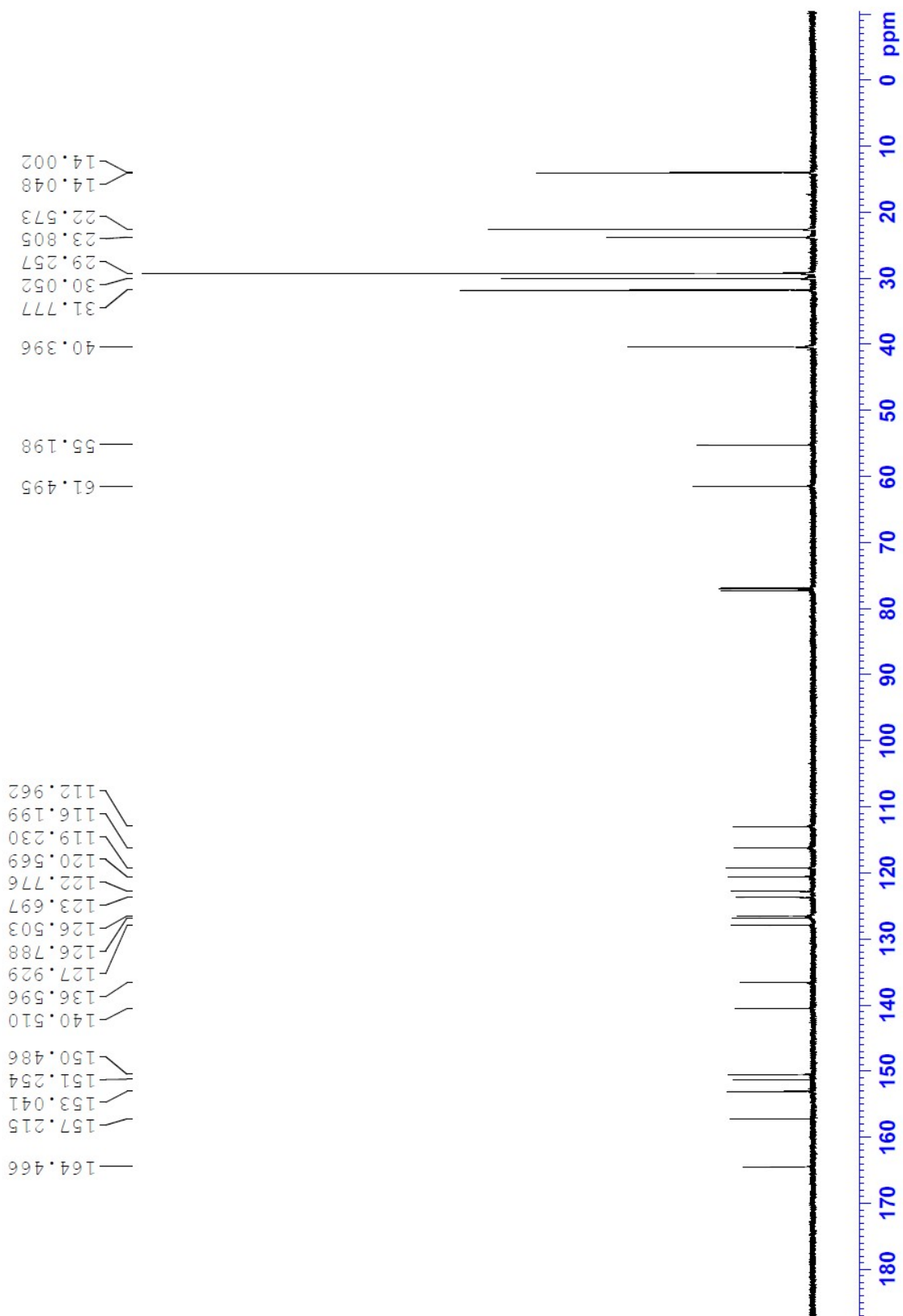


Figure S 2 ^{13}C NMR spectra of diethyl 2,5-bis((9,9-dioctyl-9H-fluoren-2-yl)oxy)terephthalate 3.

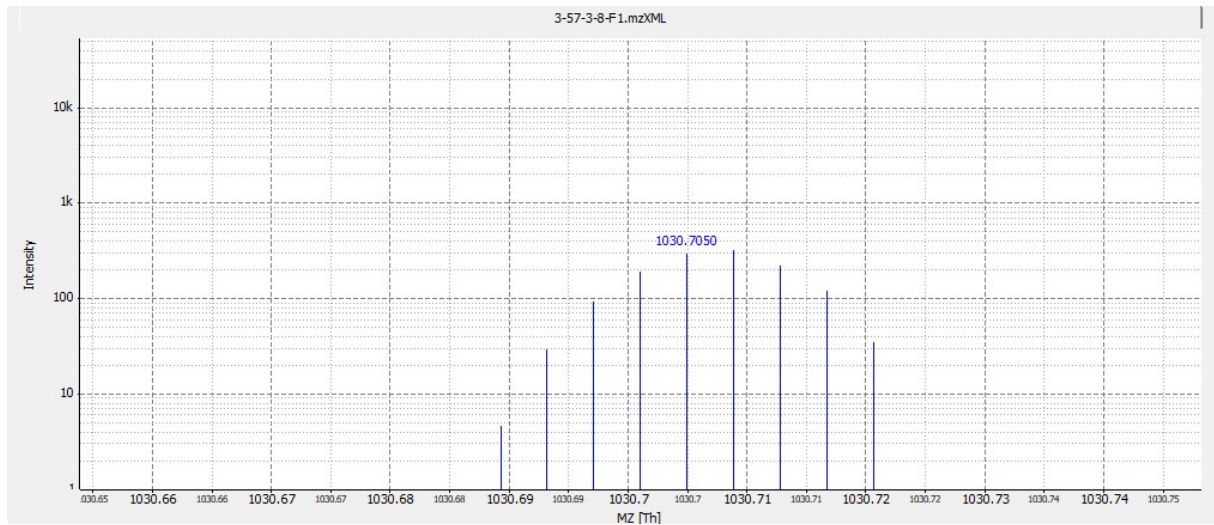


Figure S 3 HRMS spectra of diethyl 2,5-bis((9,9-dioctyl-9H-fluoren-2-yl)oxy)terephthalate 3.

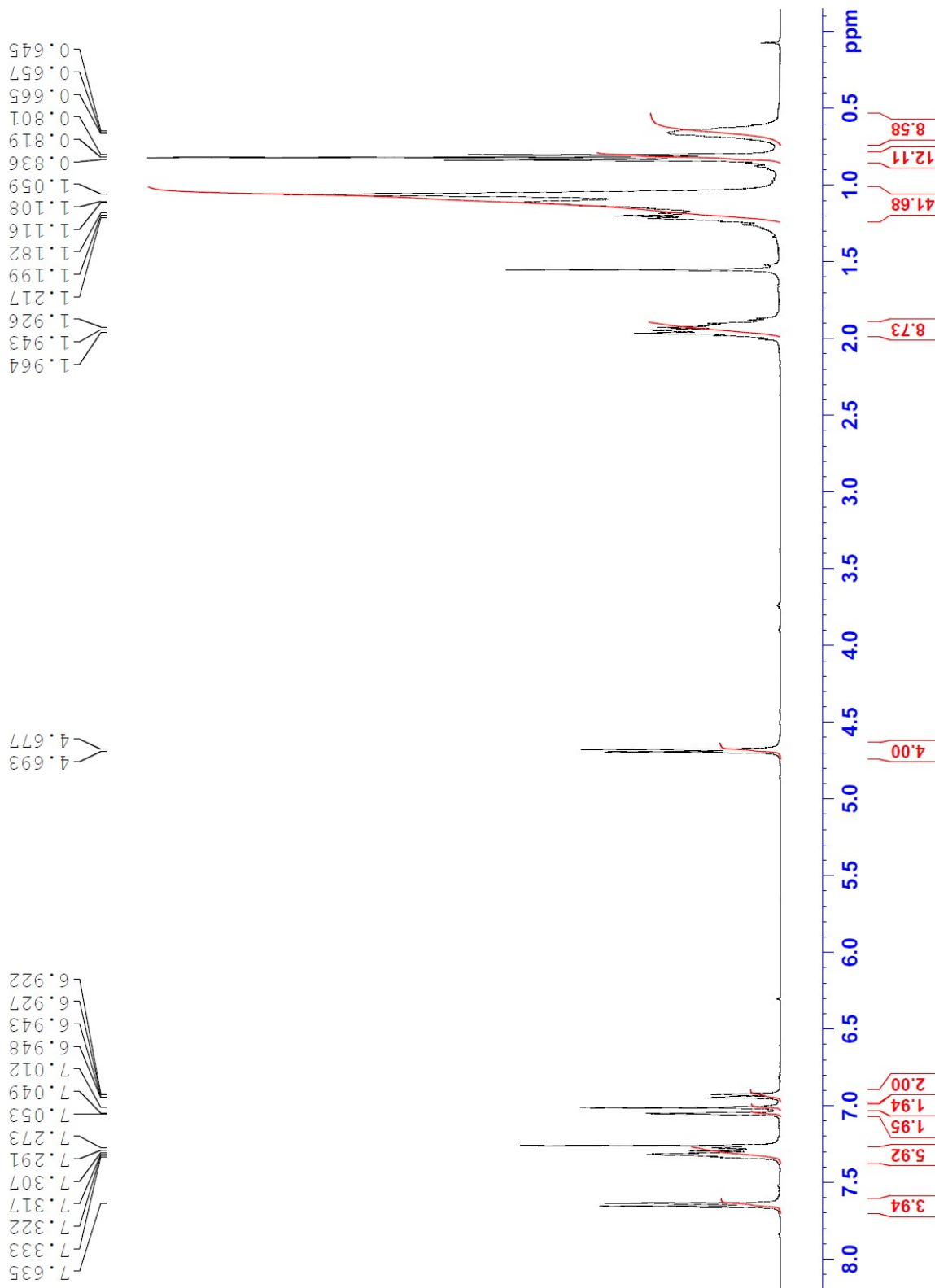


Figure S 4 ¹H NMR spectra of (2,5-bis((9,9-dioctyl-9H-fluoren-2-yl)oxy)-1,4-phenylene)dimethanol 4.

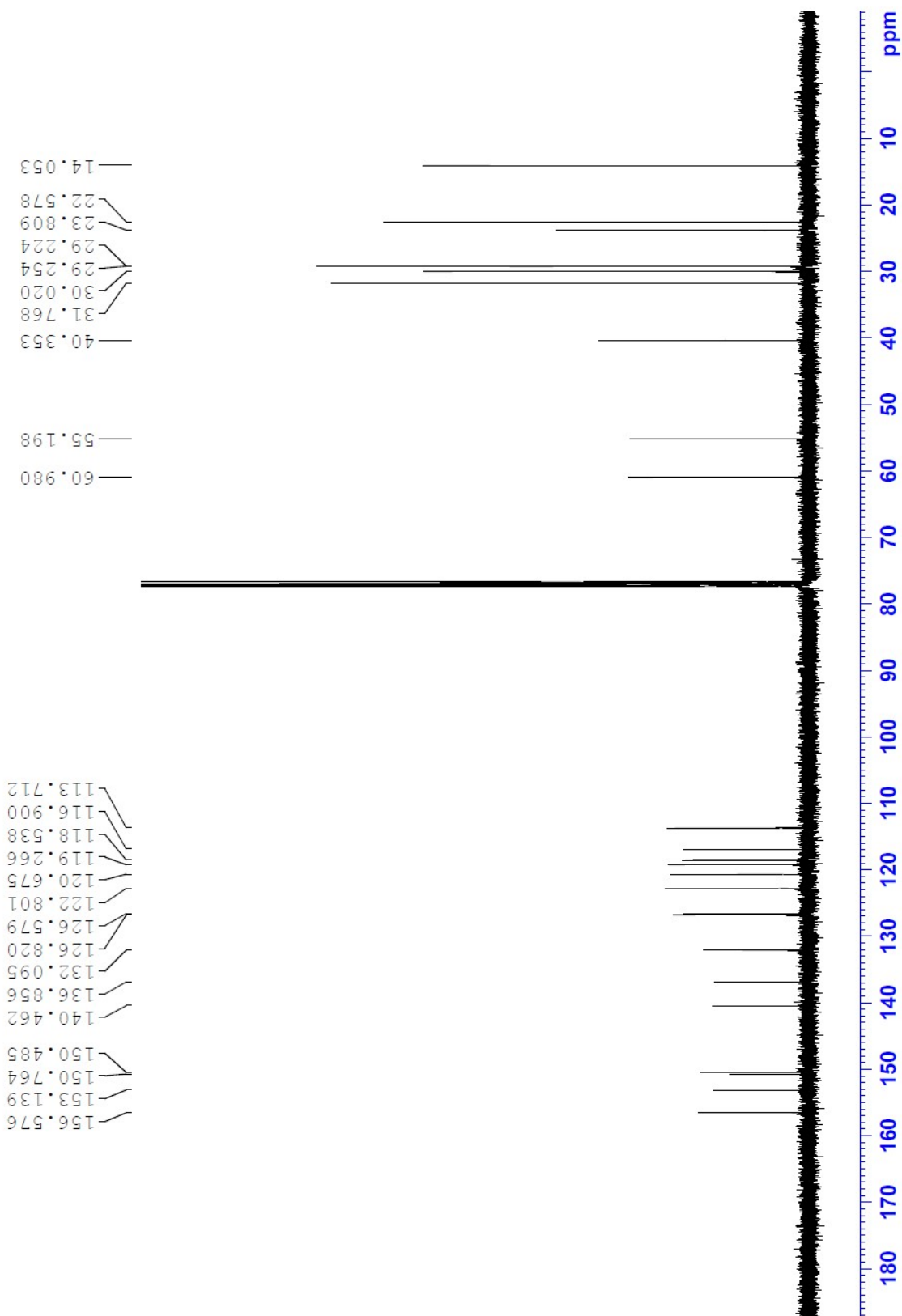


Figure S 5 ^{13}C NMR spectra of (2,5-bis((9,9-dioctyl-9H-fluoren-2-yl)oxy)-1,4-phenylene)dimethanol 4.

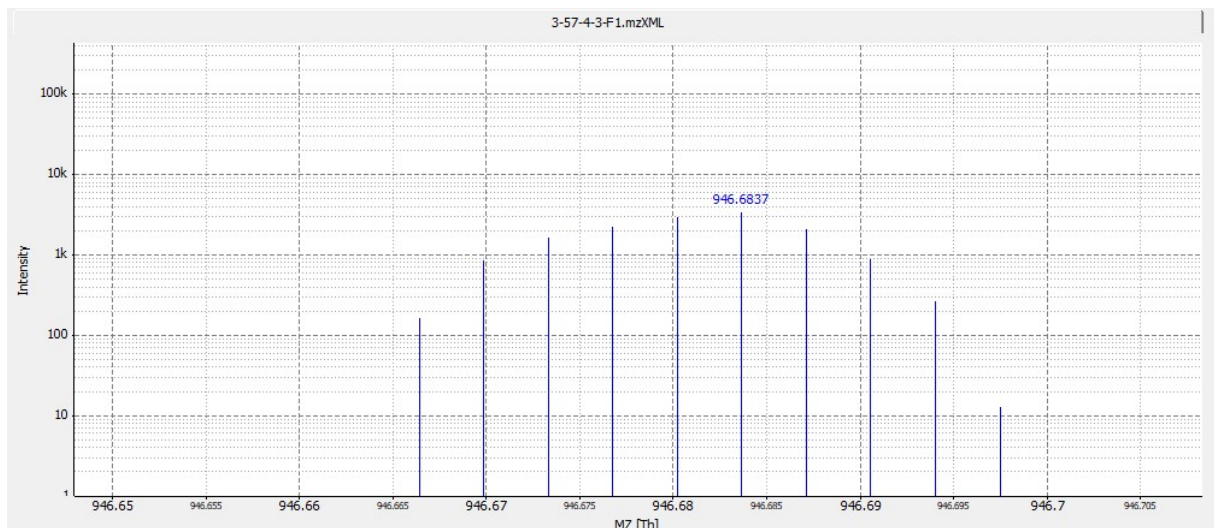


Figure S 6 HRMS spectra of (2,5-bis((9,9-dioctyl-9H-fluoren-2-yl)oxy)-1,4-phenylene)dimethanol 4.

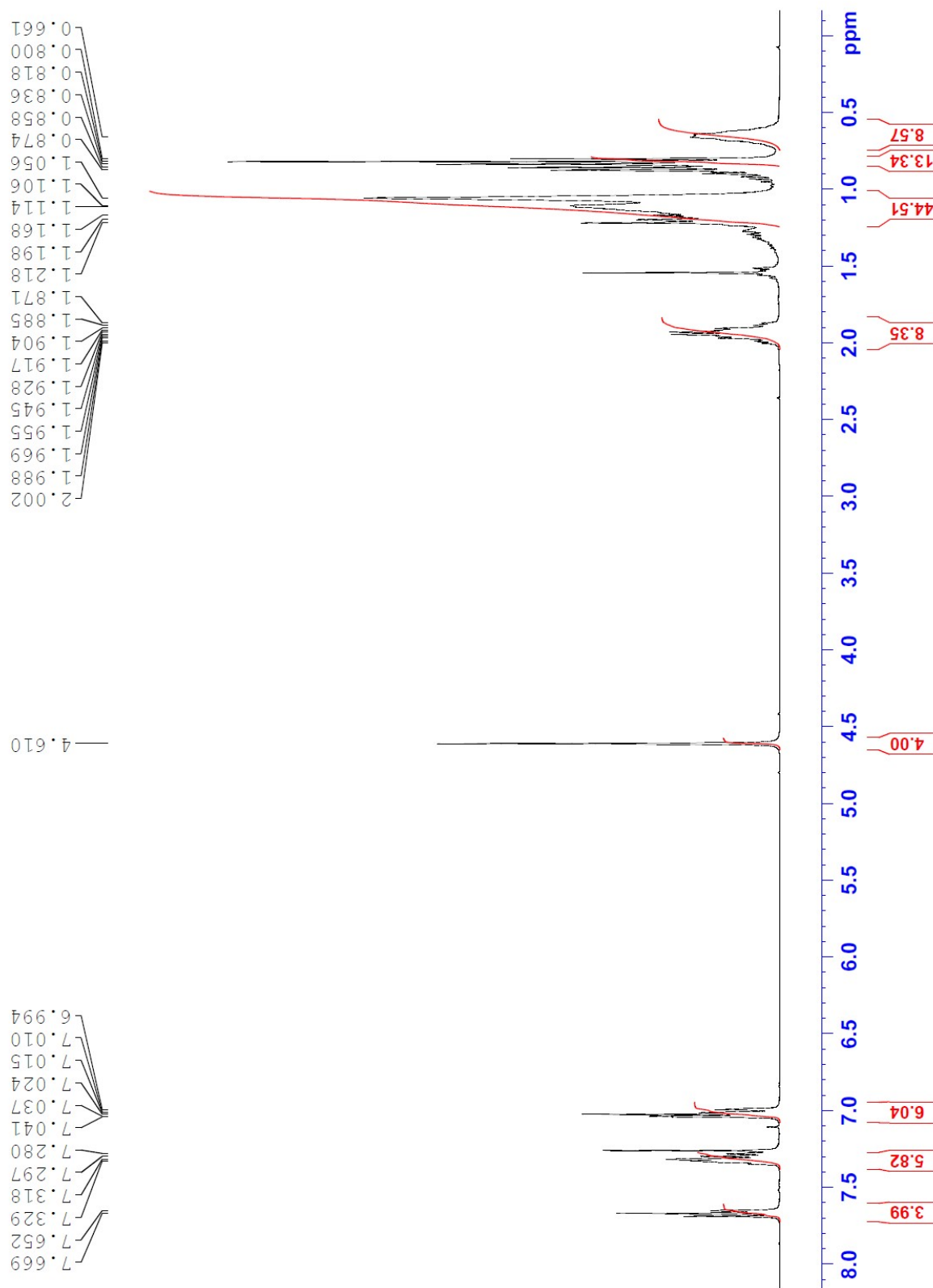


Figure S 7 ^1H NMR spectra of 2,2'-((2,5-bis(chloromethyl)-1,4-phenylene)bis(oxy))bis(9,9-diocyl-9H-fluorene) 5.

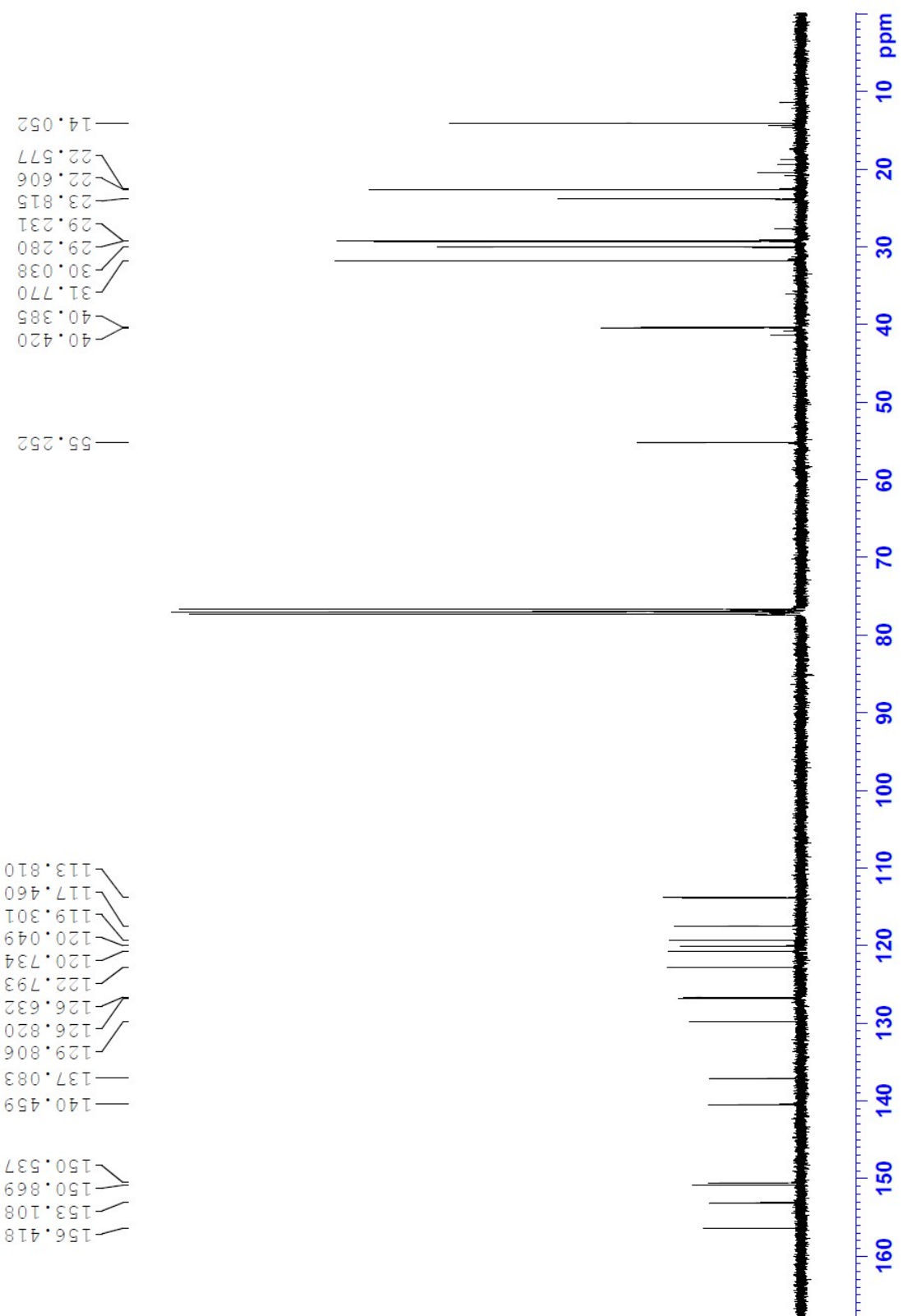


Figure S 8 ^{13}C NMR spectra of 2,2'-((2,5-bis(chloromethyl)-1,4-phenylene)bis(oxy))bis(9,9-dioctyl-9H-fluorene) **5**.

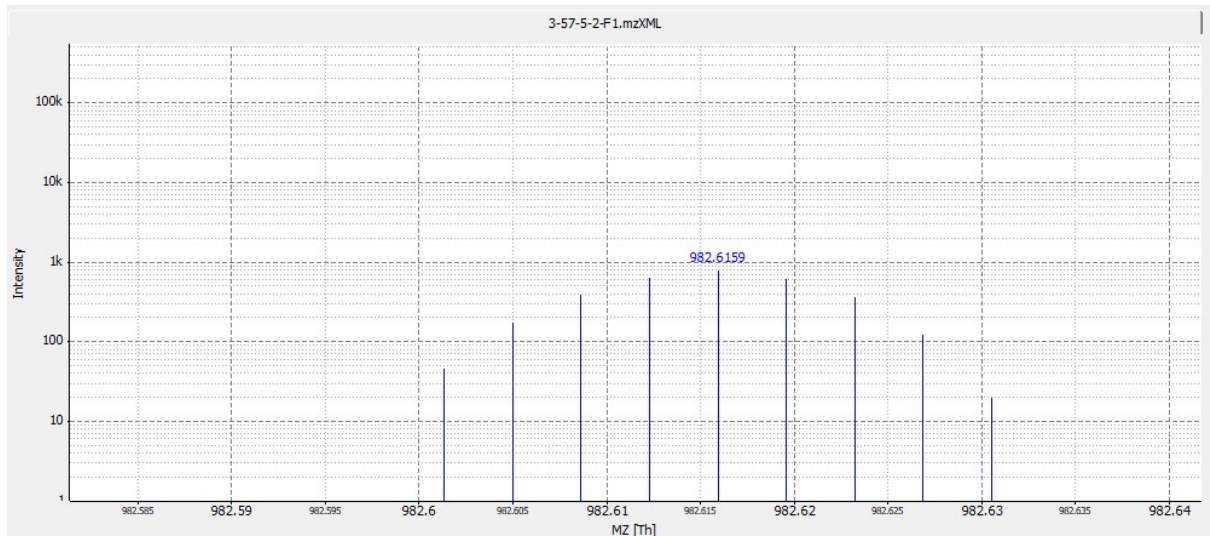


Figure S 9 HRMS spectra of 2,2'-(*[(2,5-bis(chloromethyl)-1,4-phenylene)bis(oxy)]bis(9,9-dioctyl-9H-fluorene)*) **5**.

2. Xray crystallography

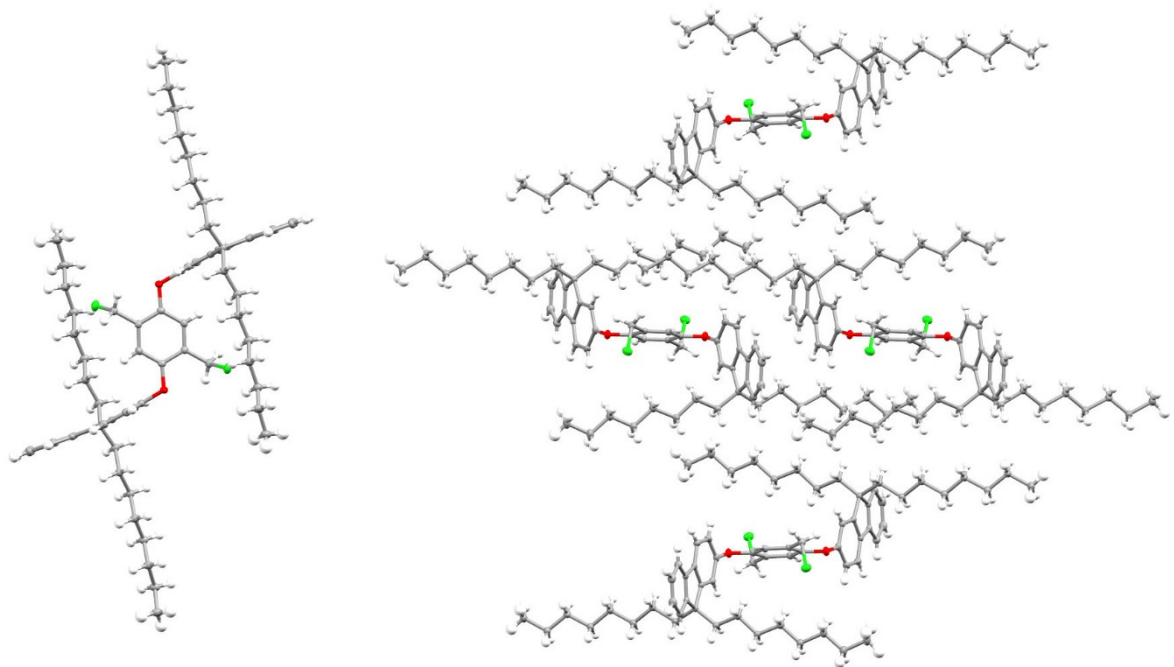


Figure S 10 Single crystal structure of 2,2'-(2,5-bis(chloromethyl)-1,4-phenylene)bis(oxy))bis(9,9-diethyl-9H-fluorene) 5.

Table S 1. Crystal data and structure refinement for 2,2'-(2,5-bis(chloromethyl)-1,4-phenylene)bis(oxy))bis(9,9-dioctyl-9H-fluorene) **5**.

Identification code	shelx	
Empirical formula	C ₆₆ H ₈₈ Cl ₂ O ₂	
Formula weight	984.26	
Temperature	100.0(1) K	
Wavelength	1.54184 Å	
Crystal system	Monoclinic	
Space group	P 21/n	
Unit cell dimensions	a = 8.3177(2) Å	α= 90°.
	b = 13.7929(3) Å	β= 91.326(2)°.
	c = 24.6719(5) Å	γ = 90°.
Volume	2829.73(11) Å ³	
Z	2	
Density (calculated)	1.155 Mg/m ³	
Absorption coefficient	1.348 mm ⁻¹	
F(000)	1068	
Crystal size	0.440 x 0.370 x 0.194 mm ³	
Theta range for data collection	3.584 to 77.160°.	
Index ranges	-10<=h<=10, -16<=k<=17, -30<=l<=31	
Reflections collected	19345	
Independent reflections	5833 [R(int) = 0.0624]	
Completeness to theta = 67.684°	99.5 %	
Absorption correction	Semi-empirical from equivalents	
Max. and min. transmission	1.00000 and 0.39095	
Refinement method	Full-matrix least-squares on F ²	
Data / restraints / parameters	5833 / 0 / 318	
Goodness-of-fit on F ²	1.058	
Final R indices [I>2sigma(I)]	R1 = 0.0521, wR2 = 0.1417	
R indices (all data)	R1 = 0.0581, wR2 = 0.1482	
Extinction coefficient	n/a	
Largest diff. peak and hole	0.249 and -0.501 e.Å ⁻³	

Table S 2. Atomic coordinates ($\times 10^4$) and equivalent isotropic displacement parameters ($\text{\AA}^2 \times 10^3$) for 2,2'-(2,5-bis(chloromethyl)-1,4-phenylene)bis(oxy)bis(9,9-dioctyl-9H-fluorene) **5**. U(eq) is defined as one third of the trace of the orthogonalized U_{ij} tensor.

	x	y	z	U(eq)
C(1)	3544(2)	9512(1)	4897(1)	18(1)
C(2)	4973(2)	8994(1)	4983(1)	17(1)
C(3)	6410(2)	9478(1)	5082(1)	19(1)
C(4)	1998(2)	9002(1)	4764(1)	21(1)
C(5)	6259(2)	7482(1)	4876(1)	20(1)
C(6)	6670(2)	7322(1)	4340(1)	19(1)
C(7)	8112(2)	6856(1)	4244(1)	17(1)
C(8)	8858(2)	6610(1)	3702(1)	18(1)
C(9)	10513(2)	6253(1)	3890(1)	18(1)
C(10)	11802(2)	5991(1)	3576(1)	22(1)
C(11)	13224(2)	5686(1)	3836(1)	26(1)
C(12)	13345(2)	5643(1)	4396(1)	26(1)
C(13)	12058(2)	5909(1)	4714(1)	23(1)
C(14)	10639(2)	6211(1)	4456(1)	18(1)
C(15)	9126(2)	6572(1)	4679(1)	17(1)
C(16)	8648(2)	6686(1)	5211(1)	21(1)
C(17)	7198(2)	7150(1)	5308(1)	21(1)
C(18)	8940(2)	7478(1)	3313(1)	20(1)
C(19)	9799(2)	8376(1)	3528(1)	21(1)
C(20)	9848(2)	9176(1)	3104(1)	21(1)
C(21)	10504(2)	10131(1)	3319(1)	24(1)
C(22)	10531(2)	10942(1)	2901(1)	24(1)
C(23)	11070(2)	11910(1)	3138(1)	25(1)
C(24)	11122(2)	12726(1)	2726(1)	31(1)
C(25)	11591(2)	13696(1)	2976(1)	33(1)
C(26)	7913(2)	5790(1)	3406(1)	19(1)
C(27)	7656(2)	4858(1)	3725(1)	19(1)
C(28)	6966(2)	4050(1)	3366(1)	20(1)
C(29)	6674(2)	3103(1)	3661(1)	23(1)
C(30)	6123(2)	2287(1)	3280(1)	22(1)
C(31)	5836(2)	1327(1)	3566(1)	23(1)
C(32)	5421(2)	495(1)	3185(1)	24(1)
C(33)	5273(2)	-471(1)	3482(1)	29(1)
O(1)	4843(1)	7989(1)	4978(1)	22(1)
Cl(1)	825(1)	8810(1)	5362(1)	28(1)

3. Polymerization data

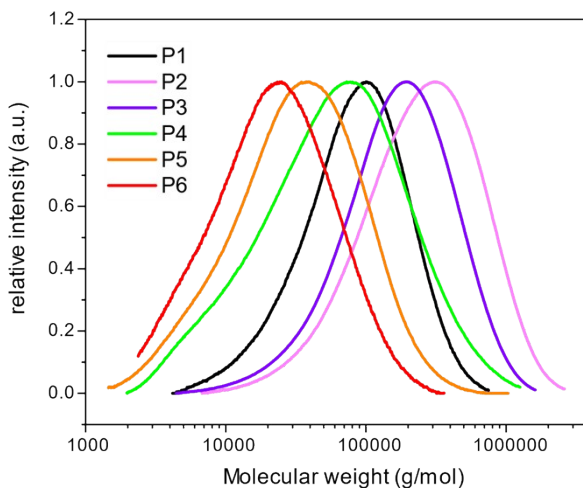


Figure S 11 GPC traces for the PPV copolymers P1-6.

Table S 3 Reaction yield for formation of PPV copolymers 7.

Monomer ratio (n:m)	Polymer yield
1:0	75%
100:1	76%
10:1	67%
1:1	59%
1:10	50%
1:100	69%

4. Density functional theory calculation

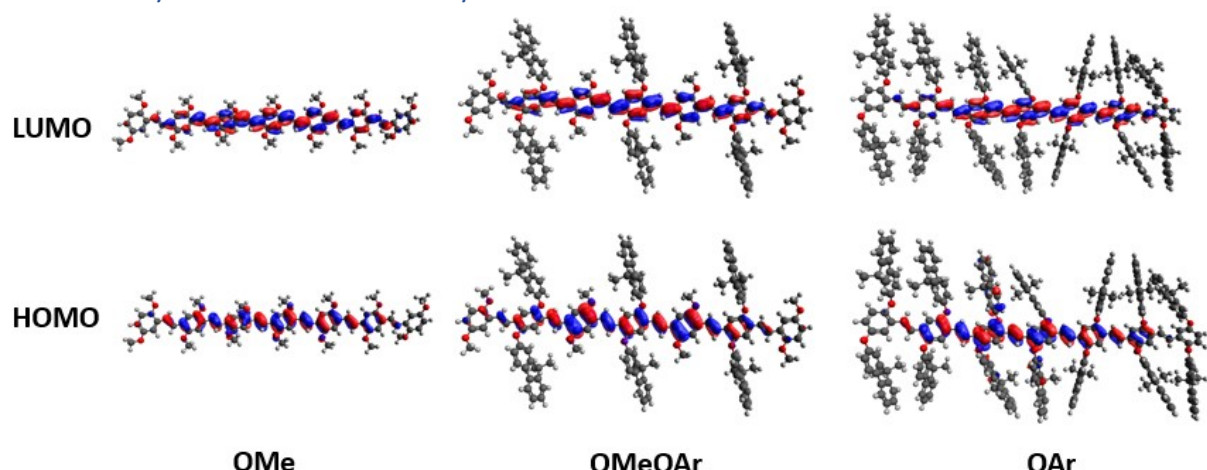


Figure S 12 TD-DFT oligomer structures showing HOMO and LUMO densities.

5. Photophysical data

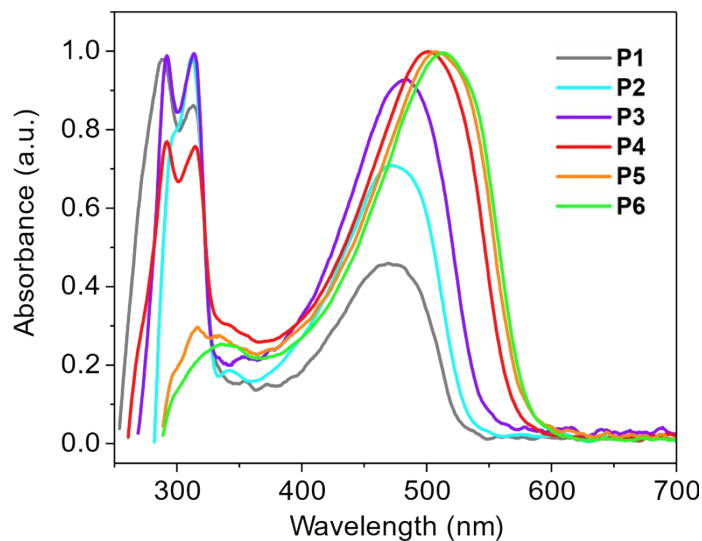


Figure S 13 Solid state UV-Vis absorbance spectra for PPV copolymers **P1-6**.

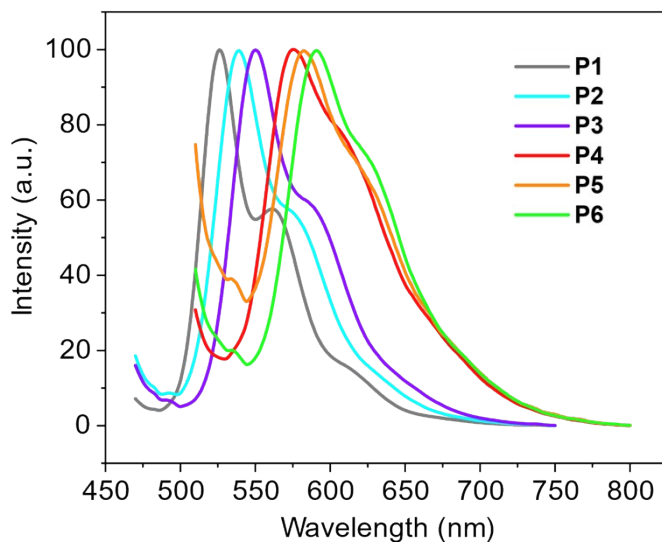


Figure S 14 Solid state photoluminescence spectra for PPV copolymers **P1-6**.

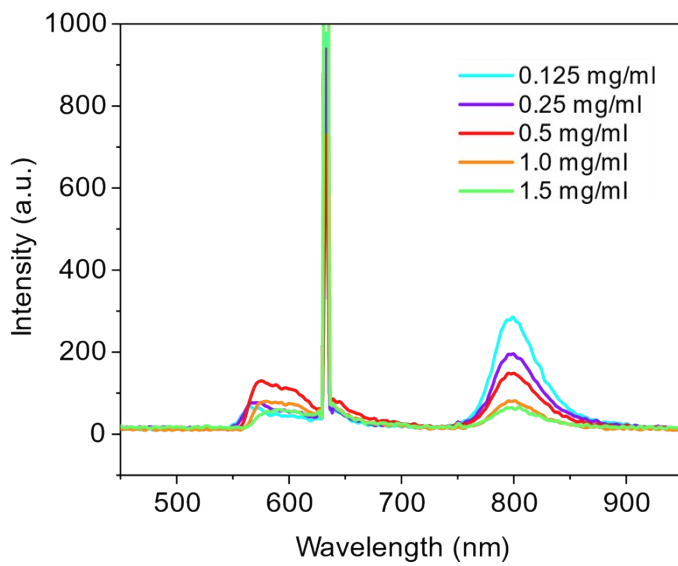


Figure S 15 Variation of PPV copolymer **P5** ($n:m = 1:10$) concentration with fixed sensitizer (PdTPTBP) concentration = 5 μM , 100 ms integration time, 632 nm excitation.

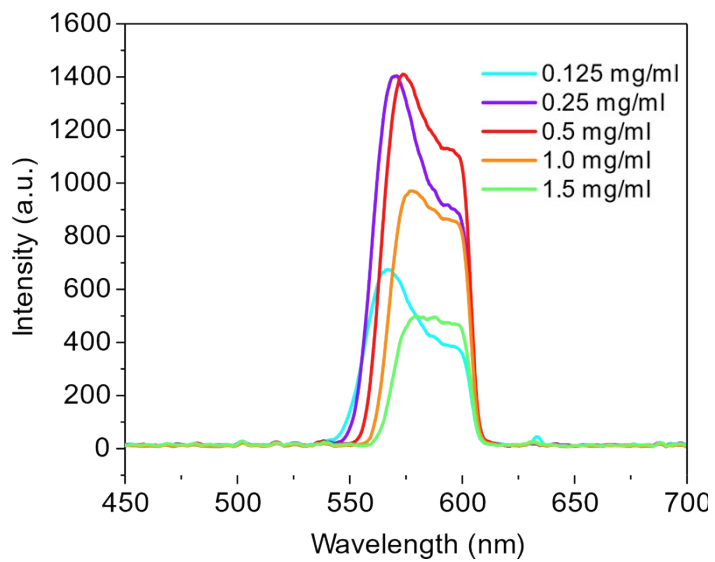


Figure S 16 Variation of PPV copolymer **P5** ($n:m = 1:10$) concentration with fixed sensitizer (PdTPTBP) concentration = 5 μM , 1000 ms integration time, 632 nm excitation, with a 600 nm low band pass filter.

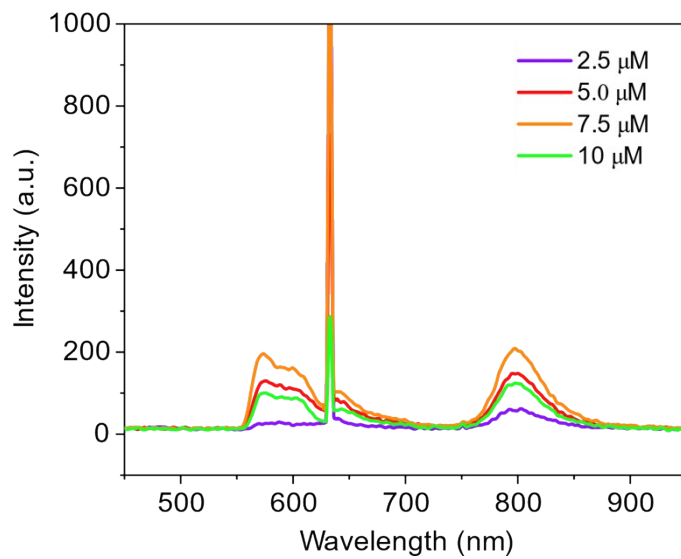


Figure S 17 Variation of sensitizer (PdTPTBP) concentration with fixed PPV copolymer **P5** (*n:m* = 1:10) concentration = 0.5 mg/mL, 100 ms integration time, 632 nm excitation.

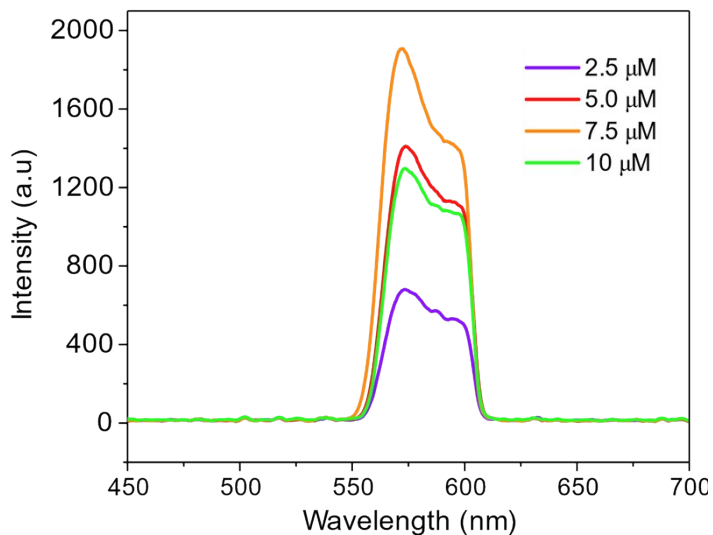


Figure S 18 Variation of sensitizer (PdTPTBP) concentration with fixed PPV copolymer **P5** (*n:m* = 1:10) concentration = 0.5 mg/mL, 1000 ms integration time, 632 nm excitation with a 600 nm low band pass filter.

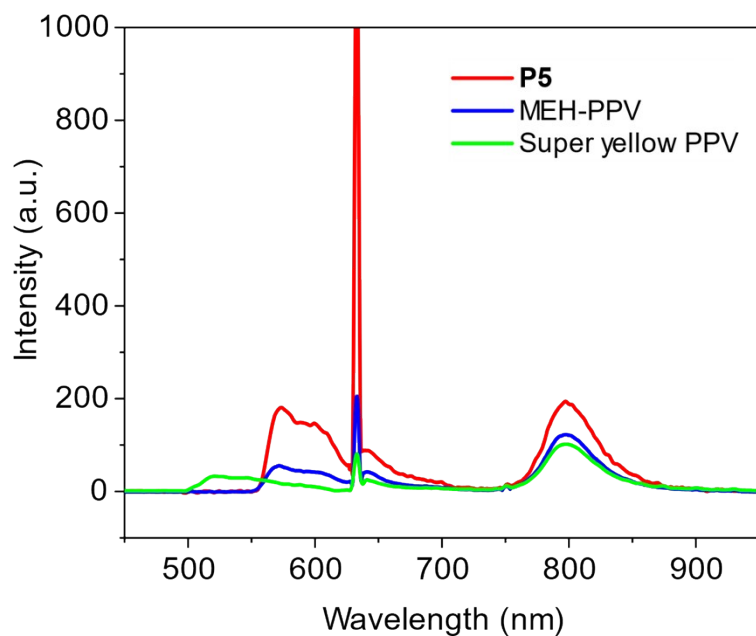


Figure S 19 Comparison of upconverted emission between PPV copolymer **P5**, MEH-PPV and Super yellow PPV with 632 nm excitation at 100 ms integration time.

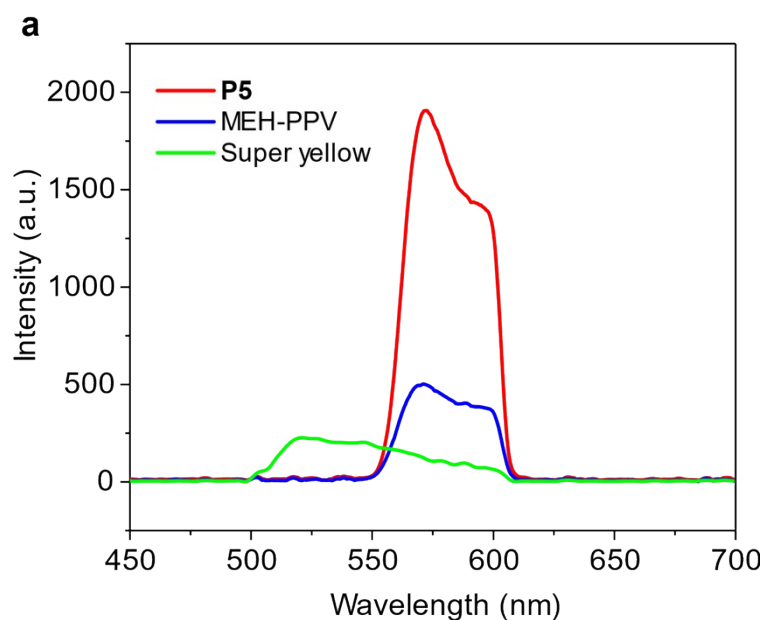


Figure S 20 Comparison of upconverted emission between PPV copolymer P5, MEH-PPV and Super yellow PPV with 632 nm excitation at 1000 ms integration time, 632 nm excitation with a 600 nm low band pass filter.

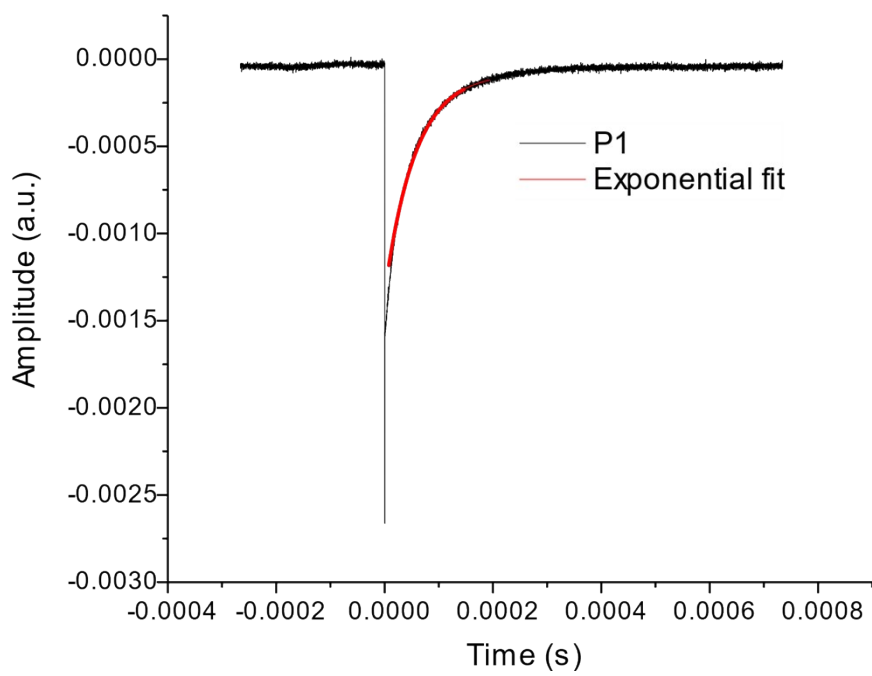


Figure S 21 Phosphorescence decay of PdTPTBP in the presence of PPV copolymer **P1** ($n:m = 1:0$), measured with 632 nm excitation and detection at 790 nm.

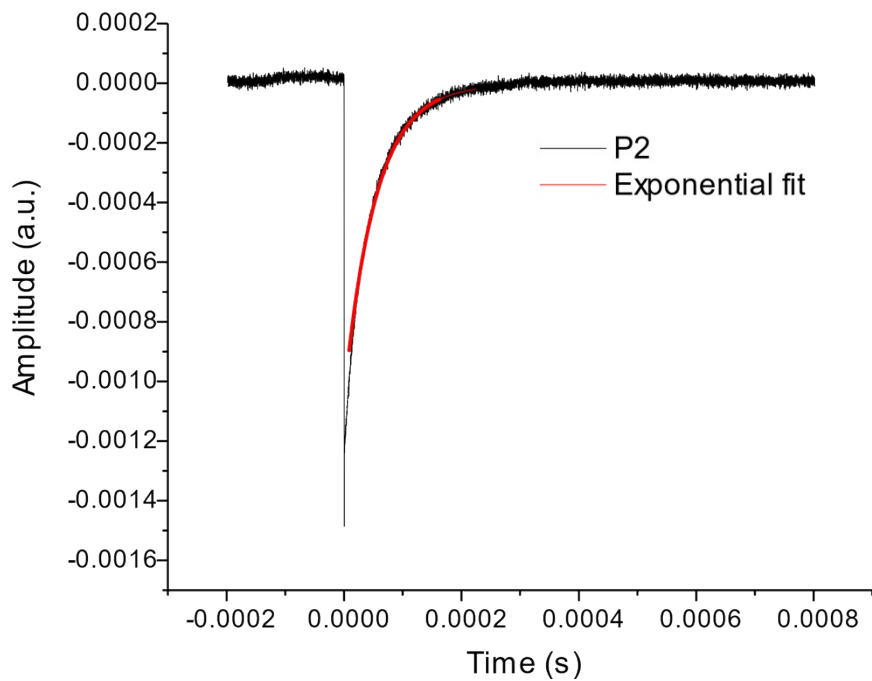


Figure S 22 Phosphorescence decay of PdTPTBP in the presence of PPV copolymer **P2** ($n:m = 100:1$), measured with 632 nm excitation and detection at 790 nm.

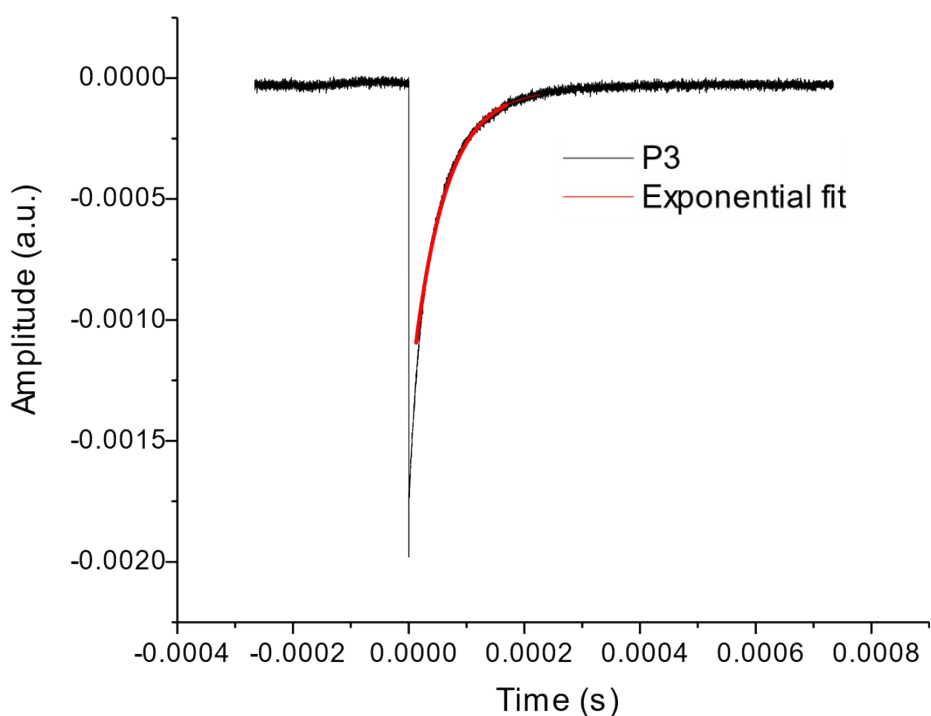


Figure S 23 Phosphorescence decay of PdTPTBP in the presence of PPV copolymer **P3** ($n:m = 10:1$), measured with 632 nm excitation and detection at 790 nm.

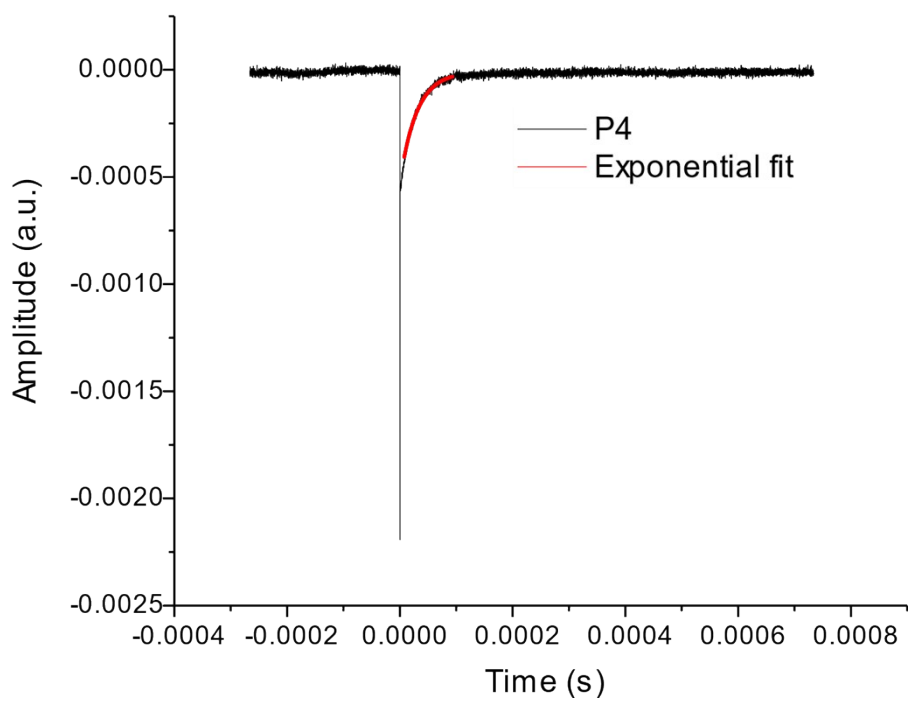


Figure S 24 Phosphorescence decay of PdTPTBP in the presence of PPV copolymer **P4** ($n:m = 1:1$), measured with 632 nm excitation and detection at 790 nm.

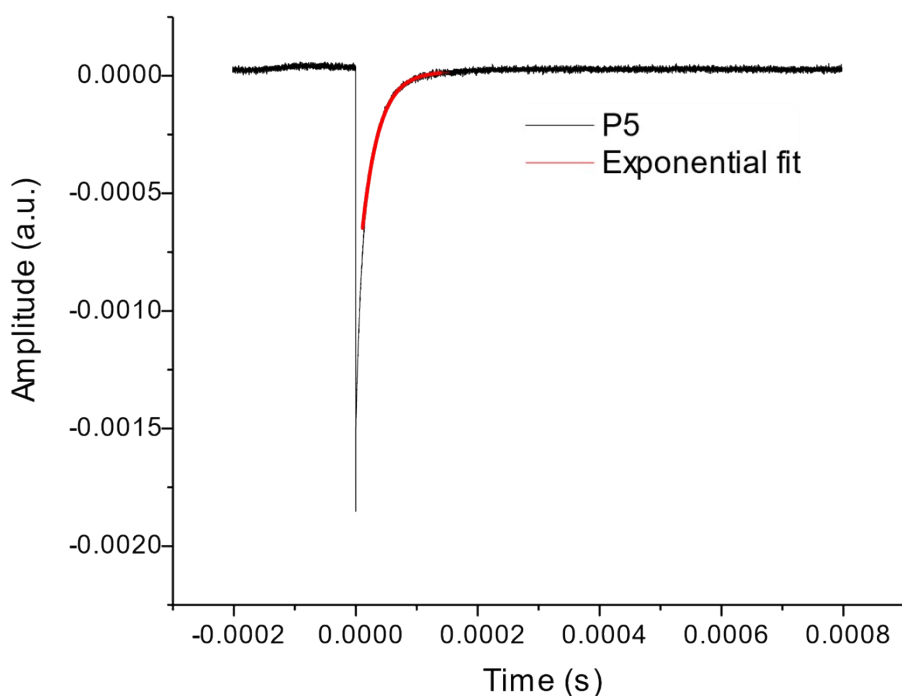


Figure S 25 Phosphorescence decay of PdTPTBP in the presence of PPV copolymer **P5** ($n:m = 1:10$), measured with 632 nm excitation and detection at 790 nm.

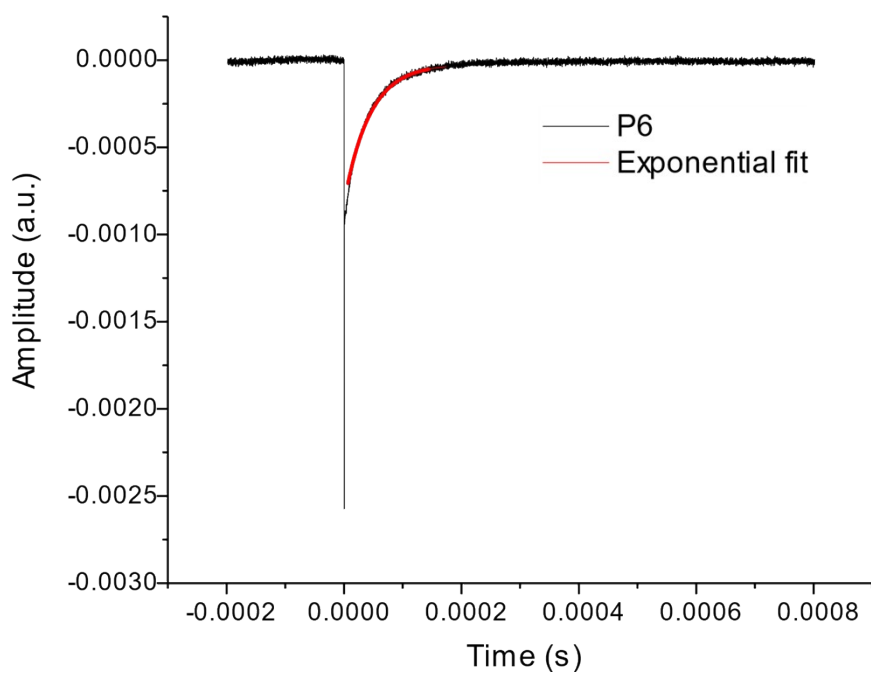


Figure S 26 Phosphorescence decay of PdTPTBP in the presence of PPV copolymer **P6** ($n:m = 1:100$), measured with 632 nm excitation and detection at 790 nm.

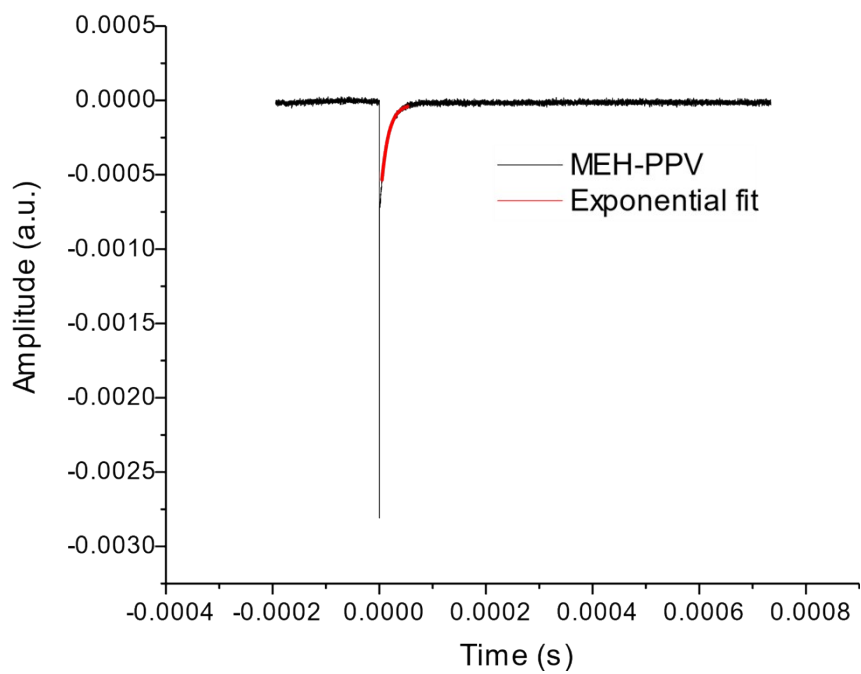


Figure S 27 Phosphorescence emission decay of PdTPTBP in the presence of MEH-PPV, measured with 632 nm excitation and detection at 790 nm.

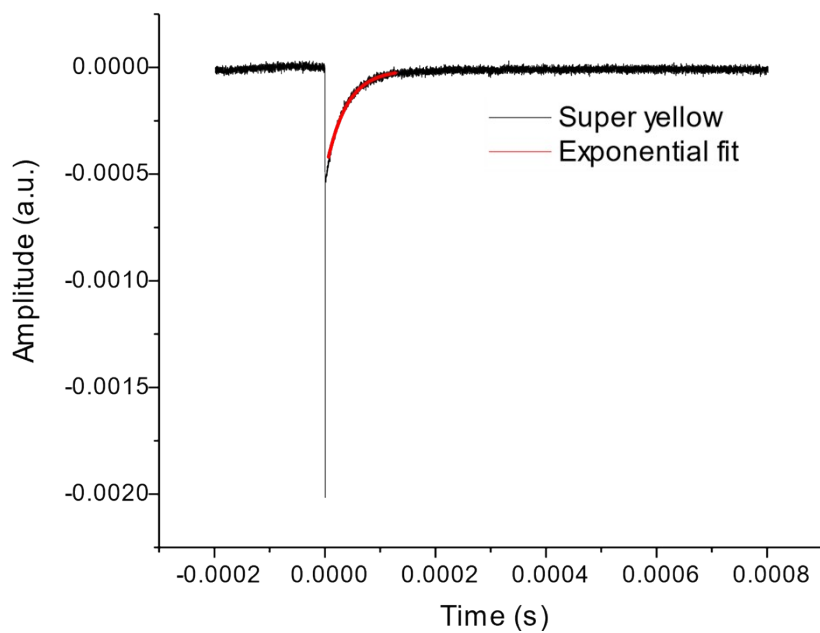


Figure S 28 Phosphorescence emission decay of PdTPTBP in the presence of Super yellow PPV, measured with 632 nm excitation and detection at 790 nm.

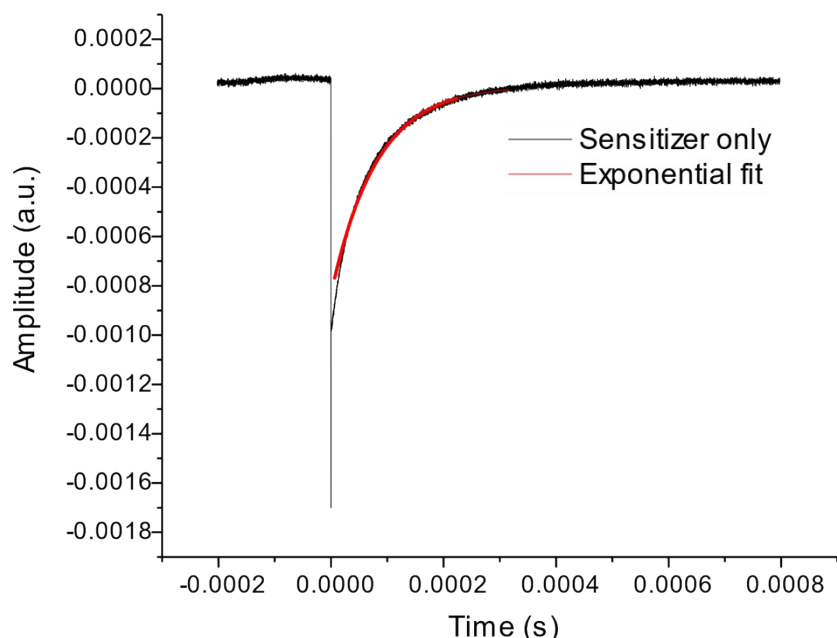


Figure S 29 Phosphorescence emission decay of PdTPTBP (sensitizer only), measured with 632 nm excitation and detection at 790 nm.

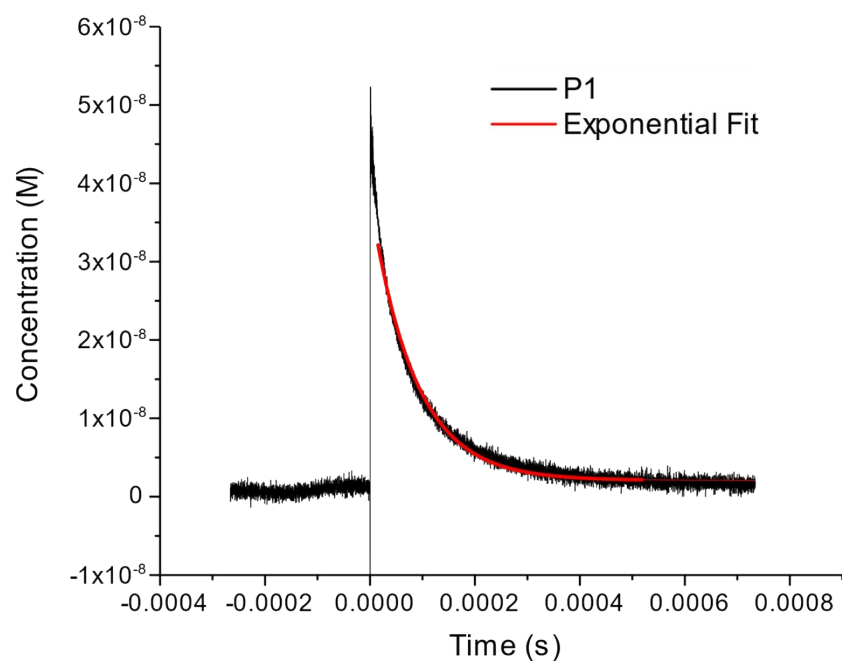


Figure S 30 Transient absorbance decay of PPV copolymer **P1** ($n:m = 1:0$) in the presence of PdTPTBP, measured with 632 nm excitation and probe at 830 nm.

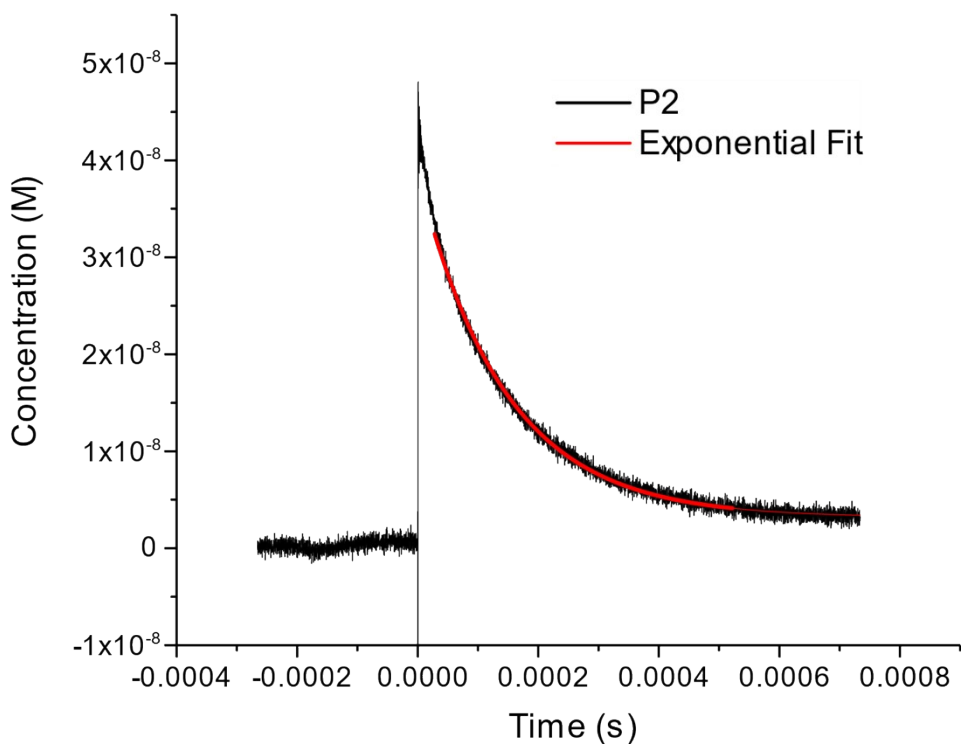


Figure S 31 Transient absorbance decay of PPV copolymer **P2** ($n:m = 100:1$) in the presence of PdTPTBP, measured with 632 nm excitation and probe at 830 nm.

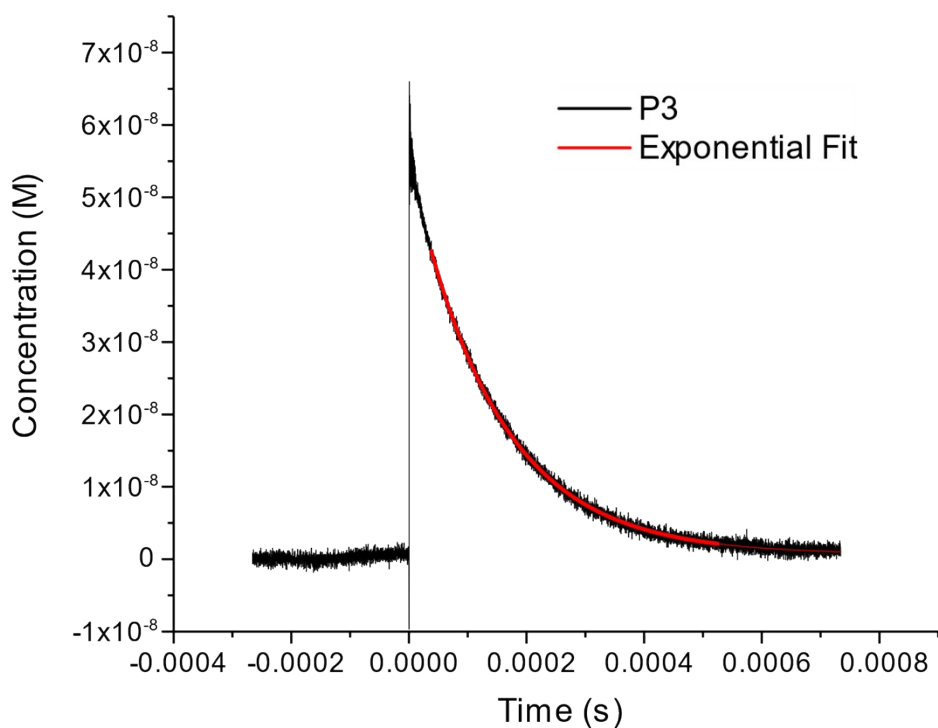


Figure S 32 Transient absorbance decay of PPV copolymer **P3** ($n:m = 10:1$) in the presence of PdTPTBP, measured with 632 nm excitation and probe at 830 nm.

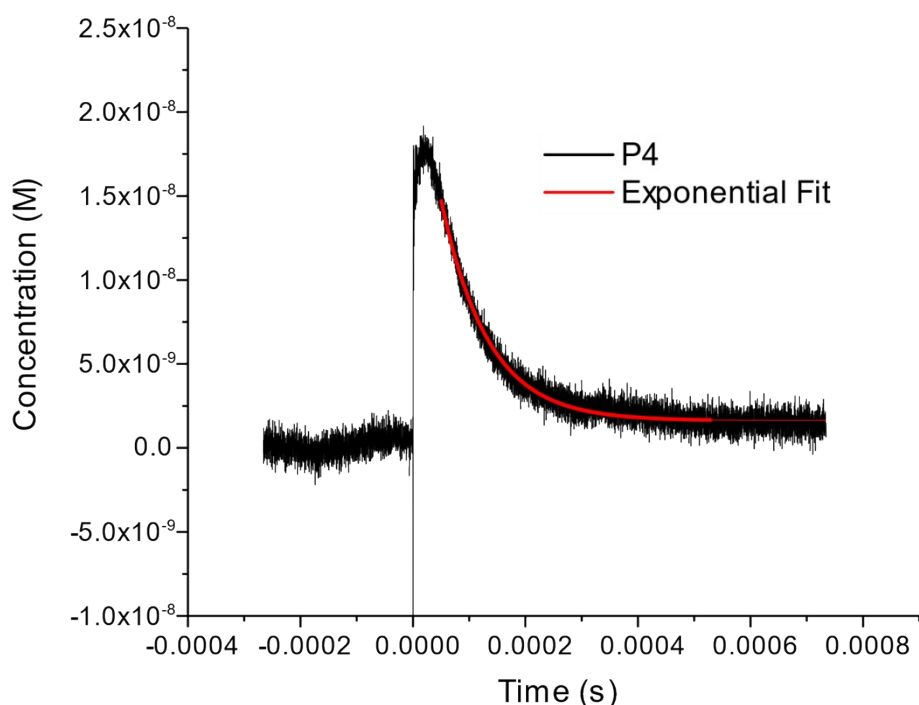


Figure S 33 Transient absorbance decay of PPV copolymer **P4** (n:m = 1:1) in the presence of PdTPTBP, measured with 632 nm excitation and probe at 830 nm.

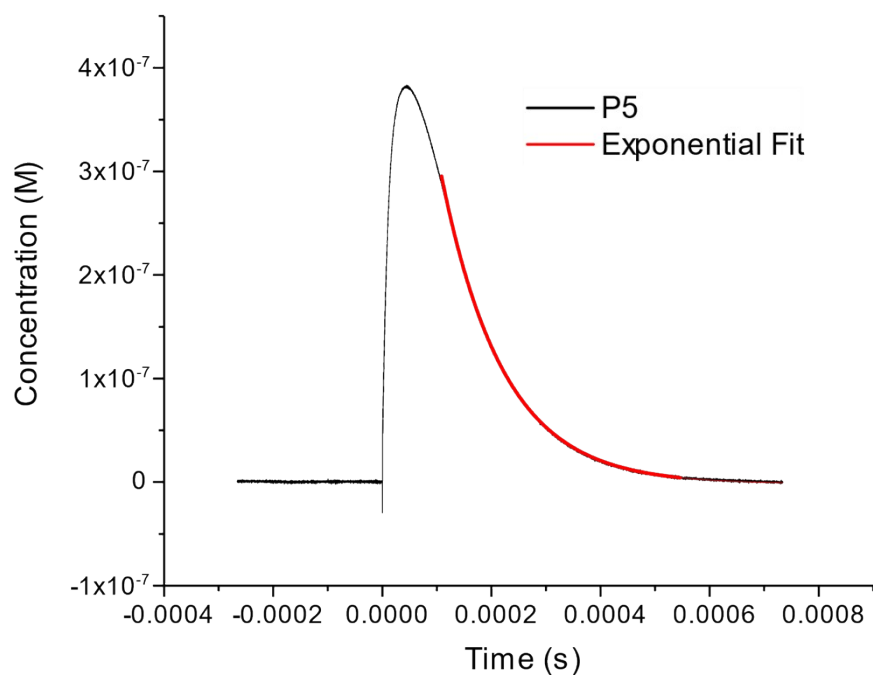


Figure S 34 Transient absorbance decay of PPV copolymer **P5** (n:m = 1:10) in the presence of PdTPTBP, measured with 632 nm excitation and probe at 830 nm.

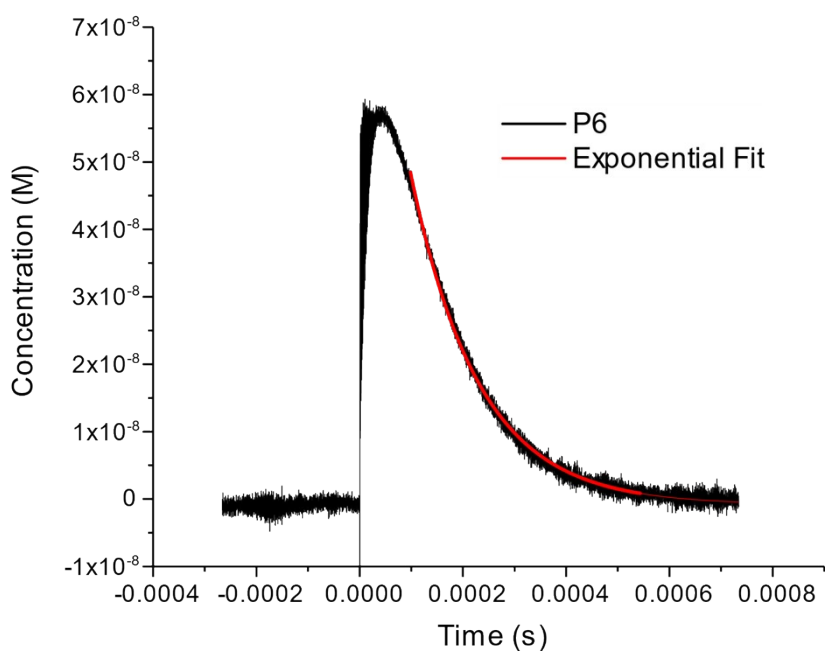


Figure S 35 Transient absorbance decay of PPV copolymer **P6** ($n:m = 1:100$) in the presence of PdTPTBP, measured with 632 nm excitation and probe at 830 nm.

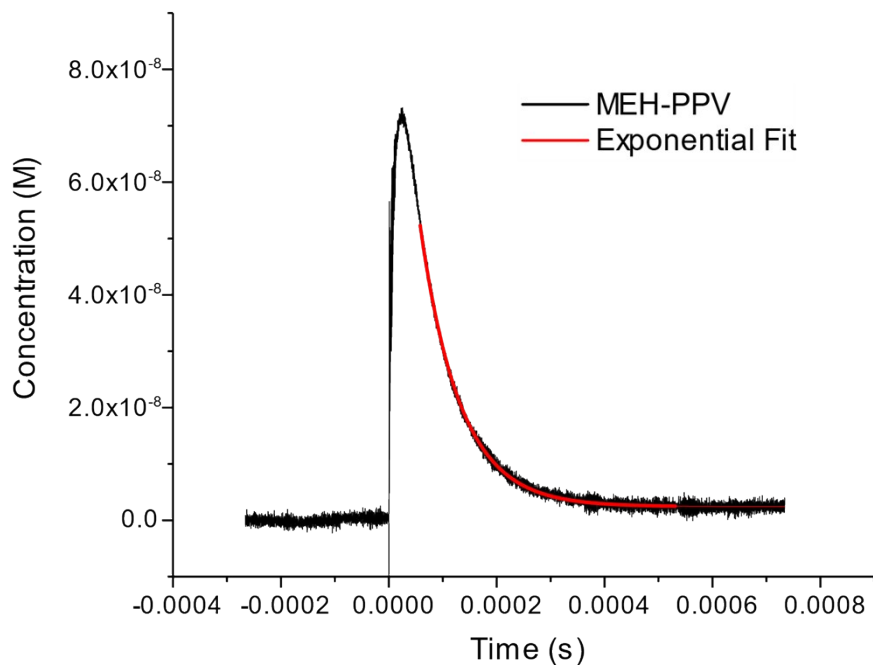


Figure S 36 Transient absorbance decay of MEH-PPV in the presence of PdTPTBP, measured with 632 nm excitation and probe at 830 nm.

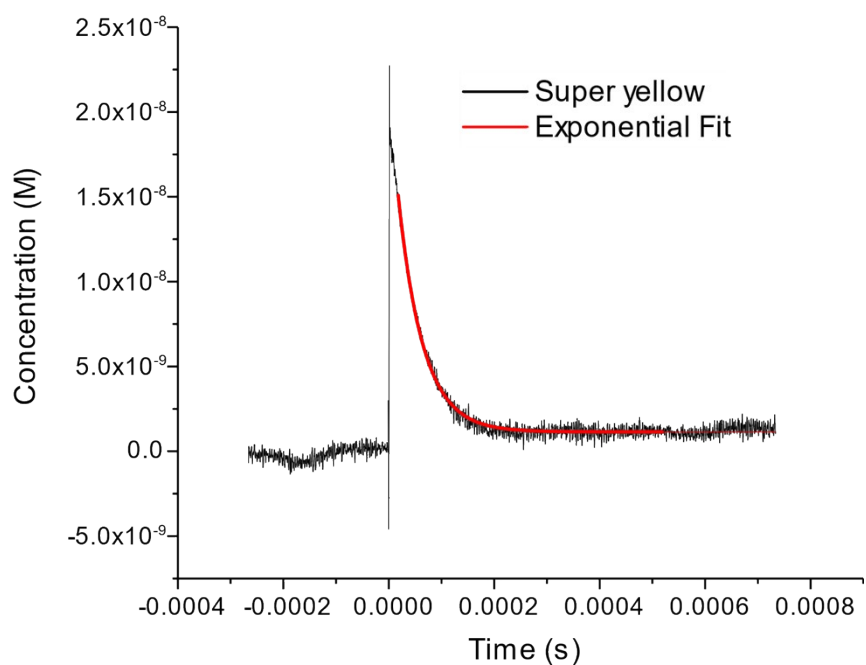


Figure S 37 Transient absorbance decay of Super yellow PPV in the presence of PdTPTBP, measured with 632 nm excitation and probe at 830 nm.